

SANDIA REPORT

SAND201X-XXXX

Unlimited Release

Printed Month and Year

Multiscale Characterization of Structural, Compositional, and Textural Heterogeneity of Nano-porous Geomaterials

Hongkyu Yoon

Prepared by
Sandia National Laboratories
Albuquerque, New Mexico 87185 and Livermore, California 94550

Sandia National Laboratories is a multimission laboratory managed and operated by National Technology and Engineering Solutions of Sandia, LLC, a wholly owned subsidiary of Honeywell International, Inc., for the U.S. Department of Energy's National Nuclear Security Administration under contract DE-NA0003525.



Sandia National Laboratories

Issued by Sandia National Laboratories, operated for the United States Department of Energy by National Technology and Engineering Solutions of Sandia, LLC.

NOTICE: This report was prepared as an account of work sponsored by an agency of the United States Government. Neither the United States Government, nor any agency thereof, nor any of their employees, nor any of their contractors, subcontractors, or their employees, make any warranty, express or implied, or assume any legal liability or responsibility for the accuracy, completeness, or usefulness of any information, apparatus, product, or process disclosed, or represent that its use would not infringe privately owned rights. Reference herein to any specific commercial product, process, or service by trade name, trademark, manufacturer, or otherwise, does not necessarily constitute or imply its endorsement, recommendation, or favoring by the United States Government, any agency thereof, or any of their contractors or subcontractors. The views and opinions expressed herein do not necessarily state or reflect those of the United States Government, any agency thereof, or any of their contractors.

Printed in the United States of America. This report has been reproduced directly from the best available copy.

Available to DOE and DOE contractors from

U.S. Department of Energy
Office of Scientific and Technical Information
P.O. Box 62
Oak Ridge, TN 37831

Telephone: (865) 576-8401
Facsimile: (865) 576-5728
E-Mail: reports@osti.gov
Online ordering: <http://www.osti.gov/scitech>

Available to the public from

U.S. Department of Commerce
National Technical Information Service
5301 Shawnee Rd
Alexandria, VA 22312

Telephone: (800) 553-6847
Facsimile: (703) 605-6900
E-Mail: orders@ntis.gov
Online order: <http://www.ntis.gov/search>



Multiscale Characterization of Structural, Compositional, and Textural Heterogeneity of Nano-porous Geomaterials

Hongkyu Yoon
Geomechanics Department
Sandia National Laboratories
P. O. Box 5800
Albuquerque, New Mexico 87185-MS0751

Abstract

The purpose of the project was to perform multiscale characterization of low permeability rocks to determine the effect of physical and chemical heterogeneity on the poromechanical and flow responses of shales and carbonate rocks with a broad range of physical and chemical heterogeneity. An integrated multiscale imaging of shale and carbonate rocks from nanometer to centimeter scales includes dual focused ion beam-scanning electron microscopy (FIB-SEM), micro computed tomography (micro-CT), optical and confocal microscopy, and 2D and 3D energy dispersive spectroscopy (EDS). In addition, mineralogical mapping and backscattered imaging with nanoindentation testing advanced the quantitative evaluation of the relationship between material heterogeneity and mechanical behavior. The spatial distribution of compositional heterogeneity, anisotropic bedding patterns, and mechanical anisotropy were employed as inputs for brittle fracture simulations using a phase field model. Comparison of experimental and numerical simulations revealed that proper incorporation of additional material information, such as bedding layer thickness and other geometrical attributes of the microstructures, can yield improvements on the numerical prediction of the mesoscale fracture patterns and hence the macroscopic effective toughness. Overall, a comprehensive framework to evaluate the relationship between mechanical response and micro-lithofacial features can allow us to make more accurate prediction of reservoir performance by developing a multi-scale understanding of poromechanical response to coupled chemical and mechanical interactions for subsurface energy related activities.

ACKNOWLEDGMENTS

This work was supported by the Sandia National Laboratories Laboratory Directed Research and Development program. The LDRD project is entitled “Multiscale Multiphysics for Subsurface Science and Engineering of Shale.” We appreciate experimental supports of Mathew Ingraham (SNL) and William Mook (SNL) for the Brazilian indirect splitting test and nano-indentation, discussion with Thomas Dewers (SNL), and computational works of Steve WaiChing Sun and SeonHong Na at Columbia University for phase field modeling. We also thank Moo Lee for his advice and support with project management.

TABLE OF CONTENTS

1.	Introduction.....	7
2.	Key Accomplishments	8
2.1.	Brazilian test of Mancos Shale and phase field modeling	8
2.2.	Nanoindentation on Mancos shale	10
2.3.	3D digital rock reconstruction	11
3.	Concluding Remarks.....	13
	References	15

FIGURES

- Figure 1. (A) A thin section image of Mancos shale with an indirect tensile test (i.e., Brazilian test). Colormap images show the mineralogy mapping obtained from the Maps Mineralogy. A backscattered scanning electron (BSE) image and a mineralogy map overlapped over the BSE image at 1 μm resolution over a small box are also shown. The last image in (A) shows the main tensile crack with the damaged surrounding fractures. (B) Progress of horizontal strain distribution based on digital image correlation during the test. Red and blue colors represent high and low strains, respectively. (C) Examples of phase field modeling in different layered cases with two components (dark and light blue for stiff and weak materials) are used. Colormap shows the phase field with the dark red as crack or highly damaged path. Image of the thin-section in (A), DIC results in (B), and modeling results in (C) are from Na et al. (2017). 9
- Figure 2. (A) Ion-polished Mancos shale (2.54cm diameter). Yellow and red areas for mineralogy mapping at 20 μm and 2 μm resolution, respectively, and BSE images at 2 μm and 0.2 μm resolution, respectively. (B) Mineralogy mapping at 20 μm resolution. Scale bar is 5000 μm . (C) SEM image of nano-indentation marks (5x5 grid) and corresponding mineralogy mapping at 2 μm scale. Four SEM images of individual indentation mark are shown. From top to bottom, clay, calcite-clay, pyrite, and calcite-dolomite-quartz-clay are dominant. (D) SEM image of indentation marks over organic matter. Red boxes show locations for 3D FIB-SEM imaging. (E) Indentation modulus (GPa) at three different scales for mineral and organic areas. Each scale has ~100 grid indentations with minerals and 50 indentations over organics. (F) SEM image of one of 1000 FIB slices. Dark region in image shows the indentation induced crack. 10

Figure 3. (A) A Selma chalk core at a depth of 6202 feet (Gulf Coast, USA). (B) Computed microtomography (microCT) image of a small sample corresponding to the thin section in (C). (C) Microscopic image of the thin section (2.5cm diameter) at 1 micron resolution. (D) Feature identification based on the spectral segmentation algorithm within a central clay seam region shown in (C). Five regions are distinctively identified in different colors. (E) Three distinct features from each of 1000 FIB-SEM image stacks representing micro-fracture (top), clay-seam (middle), and low connectivity (bottom). A total number of 15 FIB-SEM analysis were performed to characterize pore structures at 10 nm resolution based on the feature identification. (F) Multipoint statistics for digital rock reconstruction from 3D FIB-SEM images. Feature-based conditional image quilting (IQ) from segmented FIB-SEM image stack (top) is used to generate 20 realizations (1000 x 1000 x 1000) at 15 nm resolution. IQ can be also applied for small core scale (as shown in (B)) to develop digital rocks for upscaling. (G) Model dimension reduction based on the Euclidean distance measure for 100 realizations (500 x 930 x 500) at 15 nm resolution. Four clusters are used to demonstrate dimension reduction by selecting a smaller number of realizations.

..... 12

1. INTRODUCTION

Geomaterials containing nano-pores (e.g., carbonate rocks and shale) have become increasingly important for subsurface energy related activities such as geologic storage of CO₂, unconventional gas and oil recovery, and nuclear waste disposal. The coupling of geochemical reactions with hydrological and mechanical processes in nano-porous geomaterials can lead to complex behaviors involving the change of pore topology (e.g., precipitation, dissolution, compaction, fracturing) and mineralogy. As a result, these fluid-rock interactions can change hydrological, mechanical, and geophysical properties (e.g., permeability, rock strength, elastic, acoustic velocity) across spatial and temporal scales. Moreover, multiscale characteristics of textural and compositional (e.g., clay, cement, organics, microfractures, etc.) heterogeneity profoundly influence the consequences of fluid-rock interactions, resulting in the change of the mechanical properties (e.g., elastic properties, rock strength, fracture toughness). Hence, controlling fluid-rock interactions in the subsurface requires a fundamental understanding of coupled chemical and mechanical processes across scales with realistic representation of pore structure, topology, and mineralogy. This is especially true for nano-porous geomaterials because of their enormous physical and chemical heterogeneity across scales.

The objective of this work was to develop a novel integrated approach of multiscale imaging methods for mechanical and transport properties of nano-porous geomaterials with experimentation and computational modeling. For compositional and structural characterization of Mancos shales, focused ion beam-scanning electron microscopy (FIB-SEM), computed microtomography (microCT), and backscattered electron scanning (BSE) were used for a range of sample sizes. In addition, the mineralogical distribution of thin core samples polished by ion-milling was analyzed using QEMSCAN with the Maps Mineralogy. Based on mineralogy and organic matter distribution, multi-scale nanoindentation testing was performed to directly link compositional heterogeneity to mechanical properties of multiple shale samples. For carbonate chinks, two dimensional (2D) mineralogical mapping and pore structures were coupled with an array of 3D FIB-SEM analysis. FIB-SEM-EDS images of chemo-mechanically altered sample at multiple locations were used to identify distinct pore features including discrete micro-cracks in the chemically unaltered zone and sharp precipitation boundaries in the chemically altered zone. In addition, phase field modeling was used to evaluate the impact of the spatial distribution of compositional heterogeneity, anisotropic bedding patterns, and mechanical anisotropy on crack initiation and propagation during the Brazilian test of Mancos shales. Lastly, 3D digital rock reconstruction from nano- to core scales was performed with advanced multiscale image analysis for texture classification using multipoint statistics.

2. KEY ACCOMPLISHMENTS

2.1. Brazilian test of Mancos Shale and phase field modeling

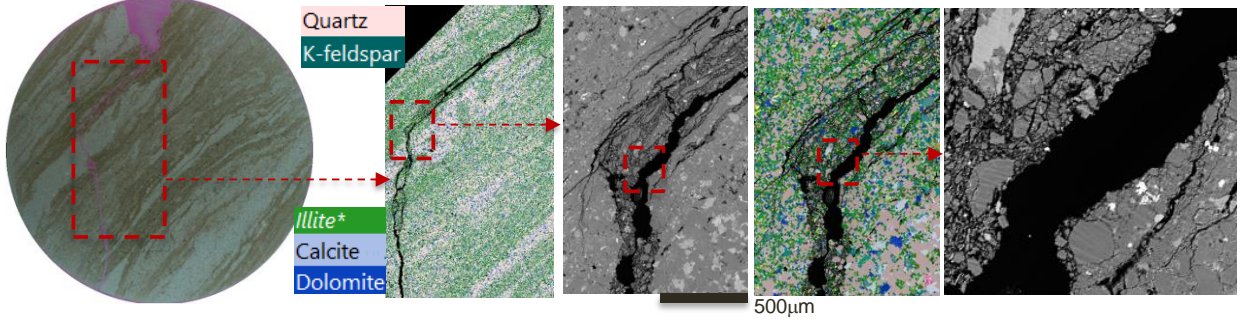
Figure 1 shows a thin-section of a Mancos shale sample after the Brazilian test (i.e., indirect tensile strength test), the mineralogical distribution of thin core sample polished by ion-milling using the MAPS Mineralogy, the lateral strain distribution during the Brazilian test, and an example of phase field modeling results. The Brazilian test of Mancos shale samples (2.5cm in diameter and 1.25cm thick) cored parallel and perpendicular to the bedding direction was performed to measure the indirect tensile strength and observe crack initiation and propagation. After testing, thin sections and billets were prepared to analyze the fracture patterns. The detailed description of these experimental and phase field modeling results was reported in Na et al. (2017). The thin section image (Figure 1A) shows the tensile strain occurred near the loading points (top area filled with a pink epoxy) at first, and then slid along the clay-rich micro-lithoface (brownish color in a thin section) adjacent to the stiff sandy micro-lithoface (bright color in a thin section). This is clearly shown in the mineralogy mapping from the Maps Mineralogy with clay-rich layers (mostly illite and illite-smectite). The Maps Mineralogy is a new FEI mineralogy analysis tool useful for high resolution images over large areas with automated mineralogy analysis. A transition area from the crack in the clay-rich to the vertical crack is highlighted in back scattered electron image and mineralogy mapping at 1 micron resolution (Figure 1A).

The testing was equipped with the digital image correlation (DIC) system to measure the local displacement, resulting in the 2D strain fields (Figure 1B). A few examples are shown. Phase field modeling results of crack initiation and propagation under different conditions are shown in Figure 1C. Phase field models treat the interfacial zone (e.g., cracks) using a diffusive transition zone and the diffuse-interface field can be obtained via minimization of a free energy functional (Moelans et al., 2008). This diffuse-interface model allows the location, evolution, and formation of fractures to be entirely determined via the solution of a partial differential equation, which can be fully or iteratively coupled to the other important physics of the problem. This can overcome some of the difficulties inherent to discrete fracture approaches that need sharp interfaces with complex evolving topologies and explicit heuristics to govern their propagation and interaction. Here we used a 2D phase field model implemented in the Deal.II (Bangerth et al., 2007, Heister et al., 2015).

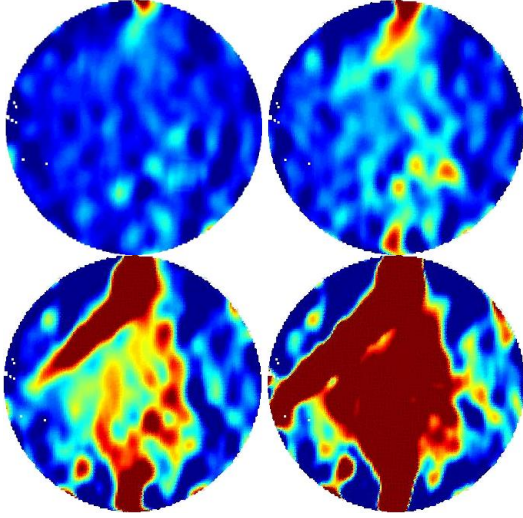
For phase field modeling shale is assumed to consist of two constituents including stiff and soft layers with the same toughness but different elastic moduli. Microstructural heterogeneity as shown in Figure 1A is simplified to represent meso-scale (e.g., millimeter scale) features such as layer orientation, thickness, volume fraction and defects. The effect of these structural attributes on the onset, propagation and coalescence of fractures was explored. Simulation results show that spatial heterogeneity and material anisotropy highly affect crack patterns and effective fracture toughness, and the elastic contrast of the two constituents significantly alters the effective toughness. Although the simplified approach couldn't account for local heterogeneity of crack initiation and propagation as shown in thin-section analysis, interaction mechanisms between the cracks using two-constituent systems were able to account for the features of elastic properties in a strongly layered system. The impact of local heterogeneity on crack initiation and propagation will be further analyzed using the mineralogical distribution (Figure 1A). For elastic properties, nano-indentation results will be utilized to develop the correlation between mineral

distribution and nano-indentation results at multiple scales. Testing with different parameterizations will demonstrate the relationship between mechanical response and microscopic features across scales, allowing us to develop a multiscale understanding of nanoporous geomaterials by correlating spatially extensible lithologic descriptions to multiscale deformation and failure.

A. A thin section of Mancos shale after Indirect tensile testing



B. Lateral strain based on digital image correlation measurements



C. Phase field modeling results (crack initiation & propagation)

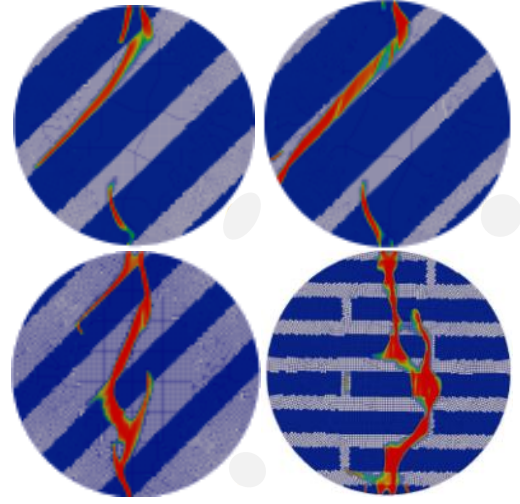


Figure 1. (A) A thin section image of Mancos shale with an indirect tensile test (i.e., Brazilian test). Colormap images show the mineralogy mapping obtained from the Maps Mineralogy. A backscattered scanning electron (BSE) image and a mineralogy map overlapped over the BSE image at 1 μm resolution over a small box are also shown. The last image in (A) shows the main tensile crack with the damaged surrounding fractures. (B) Progress of horizontal strain distribution based on digital image correlation during the test. Red and blue colors represent high and low strains, respectively. (C) Examples of phase field modeling in different layered cases with two components (dark and light blue for stiff and weak materials) are used. Colormap shows the phase field with the dark red as crack or highly damaged path. Image of the thin-section in (A), DIC results in (B), and modeling results in (C) are from Na et al. (2017).

2.2. Nanoindentation on Mancos shale

Accurate prediction of coupled chemical and mechanical processes in shale requires realistic representation of pore structure, mineralogy, and organic matters because of their physical and chemical heterogeneity across scales. Figure 2 shows an example of multiscale mineralogical mapping and nanoindentation results of a Mancos shale sample (~2.5cm diameter) which was polished by ion-milling and then scanned with BSE and MAPS Mineralogy at multiple scales. Based on mineralogy mapping, multi-scale nanoindentation testing corresponding to the peak loading of 100, 1,000, and 10,000 μN was performed to directly link compositional heterogeneity to mechanical properties in mineral and organic areas of Mancos shale (Figure 2-C&D). Nanoindentation was performed using a Hysitron Triboindenter with a Berkovich tip at a constant strain rate of 0.1 s^{-1} . The maximum load was 10 mN which was held for 5 second followed by the unloading for 10 seconds. It is noted that the surface polishing is very important to have consistent and accurate results.

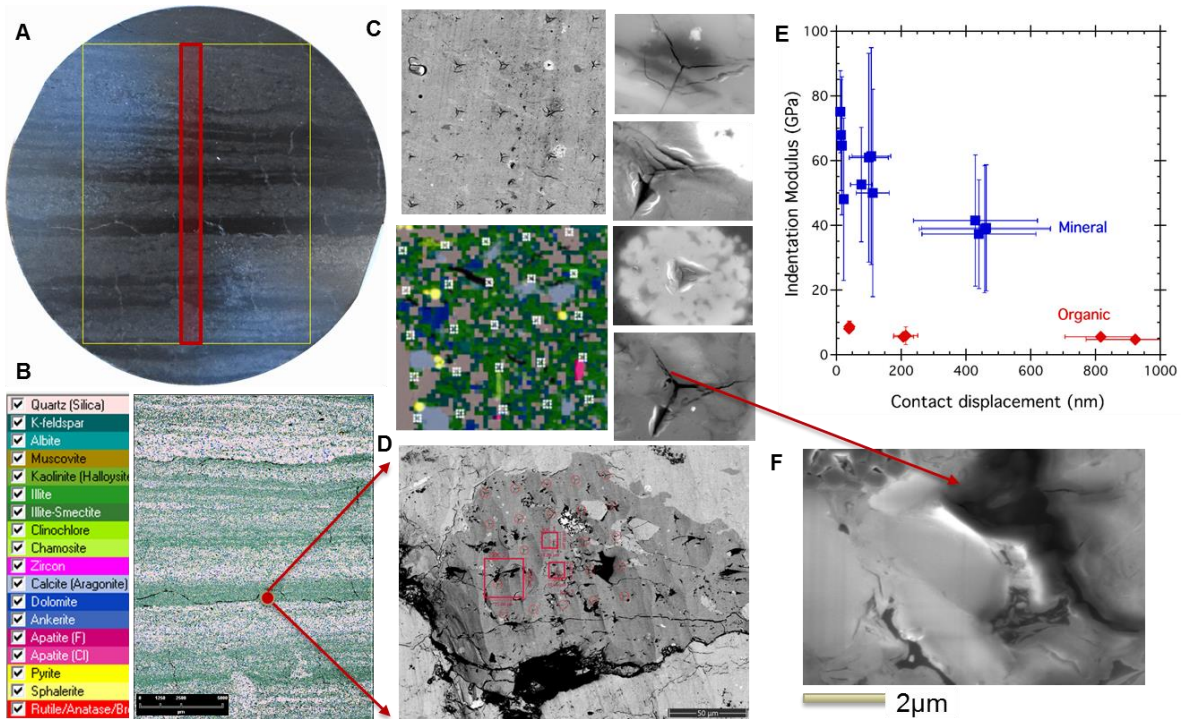


Figure 2. (A) Ion-polished Mancos shale (2.54cm diameter). Yellow and red areas for mineralogy mapping at 20 μm and 2 μm resolution, respectively, and BSE images at 2 μm and 0.2 μm resolution, respectively. (B) Mineralogy mapping at 20 μm resolution. Scale bar is 5000 μm . (C) SEM image of nano-indentation marks (5x5 grid) and corresponding mineralogy mapping at 2 μm scale. Four SEM images of individual indentation mark are shown. From top to bottom, clay, calcite-clay, pyrite, and calcite-dolomite-quartz-clay are dominant. (D) SEM image of indentation marks over organic matter. Red boxes show locations for 3D FIB-SEM imaging. (E) Indentation modulus (GPa) at three different scales for mineral and organic areas. Each scale has ~100 grid indentations with minerals and 50 indentations over organics. (F) SEM image of one of 1000 FIB slices. Dark region in image shows the indentation induced crack.

High resolution SEM images of indentation marks in Figure 2C reveal that deformation is highly influenced by the composition. Four SEM images of individual indentation mark correspond to the area with different dominant minerals consisting of clay, calcite-clay, pyrite, and calcite-dolomite-quartz-clay from top to bottom. The estimated elastic properties based on the indentation results (Figure 2E) show that indentation modulus is much widely distributed in mineral areas than in organic areas. As shown in mineralogy mapping and indentation marks in Figure 2C, the mechanical response and properties can be dramatically different depending on compositions and texture (e.g., how grains and cement coating are distributed). To further analyze the impact of pore structure on the nanoindentation results, FIB-SEM has been used to obtain 3D pore structures. One of mineral areas is shown in Figure 2F. Mechanical deformation due to indentation was quite different vertically as well. Also, permanent cracks mostly occur through cement materials between intergranular strong materials and existing defects in the vertical direction also impacted the mechanical response. These results clearly demonstrate that the distribution of pore structure and mineralogy significantly impacts the mechanical and permeability of shale. Hence, it is very critical to characterize the change of multiscale pore structure associated with chemical reactions and mechanical deformation altogether.

2.3. 3D digital rock reconstruction

Figure 4 shows an example of multiscale imaging of pore structures in carbonate rock samples from Selma Group (Navarro Formation) chalk (e.g., Yoon and Dewers, 2013). Examples of microCT (B) and optical microscopic image of the thin section (C) show micro-fractures with clay-seams in the central region. To characterize nano-pore structure, FIB-SEM analysis was applied. Given a typical sample size of FIB-SEM analysis ($\sim 10\text{-}30\text{ }\mu\text{m}$ in each dimension), 3D characterization of nano-pores with these imaging techniques requires a tremendous scanning of samples to cover a thin section. Hence, it is necessary to identify the key features critical to processes of interest. We identify key pore and morphological structures (e.g., 5-10 key microlithofacies) at \sim micron resolution mapped over an entire thin-section using multiscale and pattern-based spectral segmentation and a “support vector machine” method (e.g., Kim et al., 2013). Key patterns identify sub-micron pore structures and variable mineralogies and organics which aren’t resolvable optically by themselves, but whose fluorescent signature is unique. With the spectral segmentation algorithm (Kim et al., 2013), a central portion of the thin section fluorescence image was segmented into five primary clustering representing main features. Microfractures can be treated as inclusion of local heterogeneity in addition to main clustering. Based on this analysis, 5-10 spots on the thin section can be selected to account for nanopore structures which cannot be resolved at the thin section scale. Figure 4E shows 3D view of distinct features based on 1000 FIB-SEM images illustrating micro-fracture, clay seams, and low porosity. This demonstrates that feature identification techniques can be used to guide sample locations for FIB-SEM analysis.

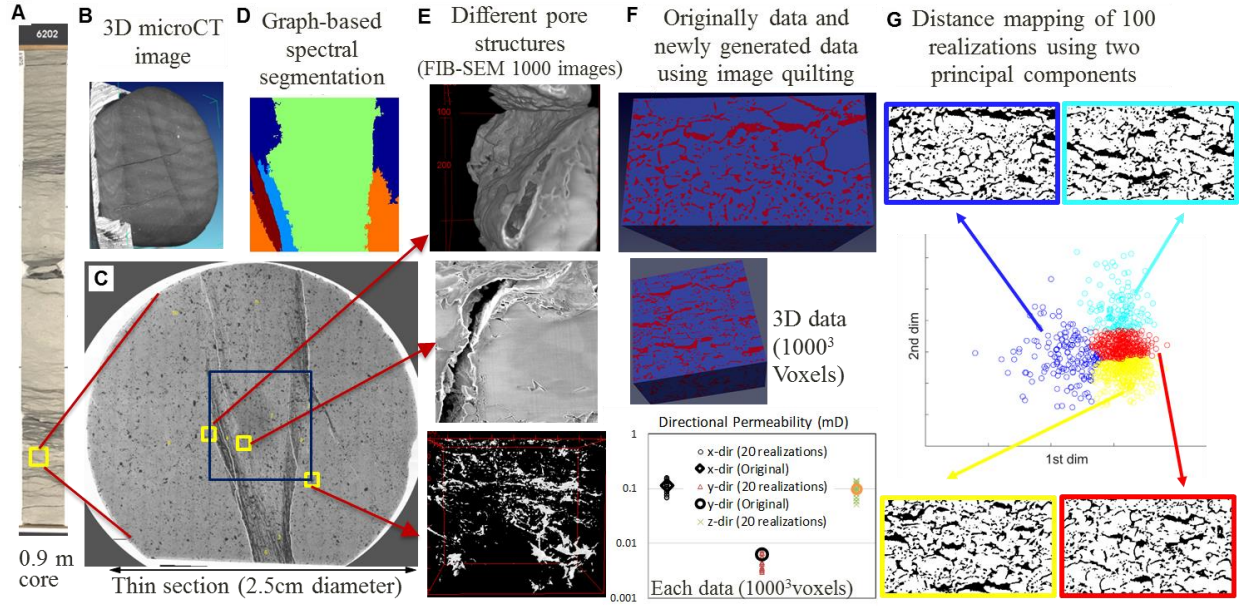


Figure 4. (A) A Selma chalk core at a depth of 6202 feet (Gulf Coast, USA). (B) Computed microtomography (microCT) image of a small sample corresponding to the thin section in (C). (C) Microscopic image of the thin section (2.5cm diameter) at 1 micron resolution. (D) Feature identification based on the spectral segmentation algorithm within a central clay seam region shown in (C). Five regions are distinctively identified in different colors. (E) Three distinct features from each of 1000 FIB-SEM image stacks representing micro-fracture (top), clay-seam (middle), and low connectivity (bottom). A total number of 15 FIB-SEM analysis were performed to characterize pore structures at 10 nm resolution based on the feature identification. (F) Multipoint statistics for digital rock reconstruction from 3D FIB-SEM images. Feature-based conditional image quilting (IQ) from segmented FIB-SEM image stack (top) is used to generate 20 realizations ($1000 \times 1000 \times 1000$) at 15 nm resolution. IQ can be also applied for small core scale (as shown in (B)) to develop digital rocks for upscaling. (G) Model dimension reduction based on the Euclidean distance measure for 100 realizations ($500 \times 930 \times 500$) at 15 nm resolution. Four clusters are used to demonstrate dimension reduction by selecting a smaller number of realizations.

With primary pore textures honored, 3D digital pore networks were reconstructed using multipoint statistical approaches. Our preliminary results with Gaussian-based approach using two-point statistics could not reproduce the long-range connectivity. In Figure 4F, one of 3D FIB-SEM image stacks was used to generate stochastic ensemble members (1000^3 voxels at 15 nm resolution) using an image quilting technique (IQ, Mahmud et al., 2014) based on the multipoint statistics. For 20 realizations porosity, correlation length, and Euler characteristics were consistent with 3D original image stack. Lattice Boltzmann simulations of 20 realizations in Figure 4 F show efficient stochastic realizations of nano-porous carbonate rock for digital rock physics. Since a large number of realizations are prohibitively expensive, we then applied a dimension reduction method to reduce the dimension of the stochastic members. Here, we applied a linear dimension reduction approach based on the Euclidean distance measure in Figure 4G. Four distinct clusters were identified. Upscaling of permeability to the Darcy scale (e.g., the thin-section scale) with image dataset can be readily achieved with this current method. We will apply non-linear dimension reduction algorithm(s) to reconstruct upscaled domain of numerical simulations with emphasis on understanding microfracture-matrix interaction, representative volume for FIB-SEM sampling, and multiphase flow and reactive transport.

3. CONCLUDING REMARKS

This project proposed a novel integration of multiscale imaging, mechanical testing, and numerical simulation to reveal the relationship between structural and mechanical response and material heterogeneity. New electron microscopy and the Maps Mineralogy have been adopted to identify multi-scale characteristics of textural and compositional heterogeneity of nano-porous shale and carbonate rocks. For compositional and structural characterization of Mancos shales, multiscale 2D and 3D imaging of pore structure and the mineralogy distribution was used to directly link compositional heterogeneity to mechanical properties from multi-scale nanoindentation testing. In addition, the spatial distribution of compositional heterogeneity, anisotropic bedding patterns, and mechanical anisotropy were employed as inputs for brittle fracture simulations using a phase field model. Comparison of experimental and numerical simulations revealed that proper incorporation of additional material information, such as bedding layer thickness and other geometrical attributes of the microstructures, will yield improvements on the numerical predictions of the mesoscale fracture patterns and hence the macroscopic effective toughness.

For carbonate rocks, multiscale imaging of pore structure and elemental and mineralogical distribution were applied for identifying the impact of chemo-mechanical coupling on the change of mineralogy, pore-structure, and mechanical properties. For example, the mineralogical mapping reveals the interface of reaction front and the textural fabrics revealed by FIB-SEM images, and elemental mapping by 3D FIB-EDS showed alteration patterns due to dissolution, precipitation, and compaction compared to unaltered sample with clear grain boundary. Combined with these results, nano-indentation testing at multiple scales will be a powerful way to evaluate the impact of the change of pore structure and mineralogy on the mechanical property. Lattice Boltzmann simulations and several analyses of characteristics of pore structures will be used to obtain permeability and multipoint statistics at several different scales. These recent advancements in multiscale imaging techniques coupled with 3D reconstruction algorithms permit development of digital rock database which will be used to evaluate the impact of rock heterogeneities such as anisotropy, pore structures, fluid distribution, and micro-fracture networks on static and dynamic poromechanical and multiphase flow properties.

During this 3-year project our technical accomplishments can be listed as:

- Performed Brazilian test of Mancos Shale and phase field modeling to evaluate the impact of elastic heterogeneity on fracture toughness. This work was published as “Na, S., W. Sun, M. D. Ingraham, and H. Yoon*, 2017, Effects of spatial heterogeneity and material anisotropy on the fracture pattern and macroscopic effective toughness of Mancos Shale in Brazilian tests, *J. Geophys. Res. Solid Earth*, 122, doi:10.1002/2016JB013374. (*corresponding author)”
- Analyzed multiscale characterization of pore structure and mineralogical distribution of nano-porous chalk and shale rocks and its impact on mechanical properties of nano-porous geomaterials
- Established a workflow to characterize morphology, mineralogy, and mechanical properties of nanoporous geomaterials across scales

- Developed an integrated approach to combine digital rock physics, experimental testing, and computational simulations for coupled chemical and mechanical responses of geomaterials
- Developed a framework for micro-structure quantification using multiscale spectral segmentation and 3D digital rock physics using multi-point statistics

In this work a comprehensive framework to evaluate the relationship between mechanical response and micro-lithofacial features was developed. Coupled with pore structure characterization, this work can reveal the scale of representative element volume for mechanical properties. Comparison of multiscale nano-indentation and core-scale mechanical testing results can reveal the significance of microscale properties in the mechanical response on the core samples. This work allows us to make more accurate prediction of reservoir performance by developing a multi-scale understanding of nanoporous materials' response to the perturbation caused by the subsurface energy activities.

REFERENCES

- Bangerth, W., R. Hartmann, and G. Kanschat, (2007), deal.II a general-purpose object-oriented finite element library, *ACM Transactions on Mathematical Software (TOMS)*, 33(4), 24.
- Heister, T., M. F. Wheeler, and T. Wick, (2015), A primal-dual active set method and predictor-corrector mesh adaptivity for computing fracture propagation using a phase-field approach, *Computer Methods in Applied Mechanics and Engineering*, 290, 466–495.
- Kim, T.H., K.M. Lee, and S.U. Lee, (2013), Learning full pairwise affinities for spectral segmentation, *Pattern Analysis and Machine Intelligence, IEEE Transactions*, 35(7), 1690-1703.
- Mahmud, K., Mariethoz, G., Caers, J., Tahmasebi, P. and Baker, A., (2014). Simulation of Earth textures by conditional image quilting. *Water Resources Research*, 50(4), 3088-3107.
- Moelans, N., B. Blanpain, and P. Wollants, (2008), An introduction to phase-field modeling of microstructure evolution, *Calphad*, 32(2), 268–294.
- Na, S., W. Sun, M. D. Ingraham, and H. Yoon, (2017), Effects of spatial heterogeneity and material anisotropy on the fracture pattern and macroscopic effective toughness of Mancos Shale in Brazilian tests, *J. Geophys. Res. Solid Earth*, 122, doi:10.1002/2016JB013374.
- Yoon, H., and Dewers, T., (2013), Characteristics of pore structures of Mississippian Selma Chalk using dual focused ion and SEM 3D imaging and lattice-Boltzmann simulations. *Geophysical Research Letters* 40, 1-5, doi:10.1002/grl.50803.

DISTRIBUTION

1	MS0751	Thomas Dewers	8864 (electronic copy)
1	MS0735	Leigh Cunningham	8862 (electronic copy)
1	MS0899	Technical Library	9536 (electronic copy)
1	MS0359	D. Chavez, LDRD Office	1911

